The International Journal of Advanced Manufacturing Technology (2018) 96:223–235
https://doi.org/10.1007/s00170-018-1586-9

ORIGINAL ARTICLE

Build orientation optimization for additive manufacturing of functionally graded material objects

Prakhar Jaiswal[1] · **Jayankumar Patel**[1] · **Rahul Rai**[1]

Received: 9 November 2017 / Accepted: 8 January 2018 / Published online: 20 January 2018

Abstract
Additive manufacturing (AM) of functionally graded material (FGM) objects has garnered significant research interest in the last decade. FGM parts printed using a 3D printer are finding innovative usages in numerous applications. To move from research sample and prototypes to commercially viable functional FGM parts, it is necessary to develop an integrated approach for modeling, optimization, and process planning for AM fabricated FGM parts. While solid modeling of FGM objects has been studied in detail, the build orientation optimization and process planning for AM fabricated FGM objects remain largely unaddressed. The build orientation of FGM object can significantly influence overall print quality and cost. In this paper, we introduce a novel approach for build orientation optimization (BOO) of additively fabricated FGM parts. The formulated BOO cost function encapsulates material error and geometric error as primary factors. The geometric error considers volumetric stair-case error and the material error accounts for errors due to the discretization of material composition across the cross-section of the toolpath. A novel multi-scale material error computation approach has been proposed to effectively and efficiently compute the material error. Since the build orientation cost function cannot be explicitly defined, and an expansive parametric sweep is too computationally expensive to implement, a surrogate model-based global optimization was implemented to solve the formulated BOO problem. The proposed optimization framework has been assessed using various test objects to illustrate the overall methodology and demonstrate its effectiveness.

Keywords Functionally graded materials · Distance-based material representation · Orientation optimization · Additive manufacturing · Multi-scale random error

1 Introduction

Functionally graded materials (FGM) are advanced materials with varying material composition, microstructure, or porosity across the volume, tailored for a specific performance or function [35]. FGMs offer great promise in areas of applications with harsh working conditions and/or extraordinary material properties requirement such as defense, aerospace, and healthcare (medicine delivery, dental/orthopedic implants) [29]. Bulk FGM parts are mainly fabricated by powder metallurgy method, centrifugal casting method, and additive manufacturing methods [24, 30, 44].

✉ Rahul Rai
rahulrai@buffalo.edu

[1] Manufacturing and Design Lab (MADLab), University at Buffalo, Buffalo, NY, USA

As the initial capital cost and the cost of raw materials for additive manufacturing is declining with each passing year, additive manufacturing of FGMs have garnered a lot of research interest in the last decade. Researchers have mainly focused on FGM modeling, material processing, and optimization of fabrication processes for FGMs. The main advantage of FGM over homogeneous material is the distribution of material composition/microstructure over its volume to accommodate conflicting and spatially varying material properties. However, to actualize this fascinating advantage, it is also important to produce the desired material distribution using a given manufacturing method with minimal error.

In layered manufacturing, build orientation choices can severely impact the material composition error. There exist several studies focusing on the impact of build orientation on surface quality, build time, and overall fabrication cost of single material (homogeneous) 3D printed part [2, 3, 8, 33]. However, there is a dearth of research focused

on studying the impact of build orientation on material composition error in additively fabricated FGM objects. This paper addresses an important research gap in the area of build orientation optimization for additive manufacturing of FGMs.

In this paper, a novel build orientation optimization framework is introduced that aims to minimize geometric error (surface quality) and material composition error for FGM objects fabricated using additive manufacturing processes like fused deposition modeling (FDM). The optimization cost function was defined as a weighted average of normalized geometric and material composition errors. Geometric error takes into account the staircase effect that degrades surface quality. Material composition error encapsulates the difference between the desired fractional composition of two or more materials at a given point and the estimated attainable fractional composition at that point. The difference in desired and attainable material composition error arises mainly due to two factors: (a) discretization along slice height (z-axis) and (b) discretization across the cross-section of toolpath (xy-plane). A novel concept of multi-scale random error has also been introduced that attempts to compute the material composition error more efficiently and accurately compared to conventional integration or grid-point-based error computations.

The primary contributions of the paper are as follows:

1. A novel optimization-based framework to formulate the build orientation optimization of additively fabricated FGM parts that encapsulates both geometric and material composition errors.
2. A novel multi-scale material error computation to compute material composition error that takes into account the contextual information around the point of error evaluation.
3. A surrogate model-based global optimization framework for solving the formulated optimization problem.

The paper is organized as follows: In Section 2, relevant literature is reviewed. The FGM modeling scheme is discussed in Section 4. The overall build orientation objective cost function formulation and computation is described in Section 5. The surrogate model-based optimization process is discussed in Section 6. Results for example test cases are presented in Section 7 to demonstrate the effectiveness of the proposed methodology. Section 8 concludes the present work with some notes on future research directions.

2 Literature survey

Extensive research literature exists in additive manufacturing (AM) related fields like computational design for AM [13, 25], AM processes [14, 15, 39], process modeling and optimization [6, 21, 37, 45], material science [1, 11], and energy and sustainability [27, 42]. However, additive manufacturing for functionally graded materials (FGMs) has only recently started attracting research interest. So far, most of the research work in FGM domain has focused on computational modeling of FGM objects. Build orientation optimization and fabrication process planning for additive manufacturing of FGM is still an understudied research topic.

Since the early 2000s, there have been many FGM representation schemes proposed to efficiently and accurately store, exchange, and process the volumetric as well as material composition information. One of the first notable work to represent FGM for layered manufacturing was done by Kumar and Dutta [9], wherein the modeling space was represented by r_m-sets and r_m-objects. Mathematical Boolean operators were also defined to facilitate modeling process. Jackson et al. [19] and Liu et al. [28] devised a finite element-based local composition control (LCC) approach that represents FGM objects as tetrahedral mesh model and material composition was evaluated for every tetrahedral node by using Bernstein polynomials. The material composition of any query point was then interpolated using material composition at the nodes of the incidental tetrahedron. Kou and Tan [26] proposed a hierarchical representation for FGM by using B-rep to represent geometry and heterogeneous feature tree to define material distribution. Gupta and Tandon [16] used material convolution surfaces to model complex FGM objects with multi-functional heterogeneity, convolution material primitives, membership functions, and material-potential functions. A review of FGM representation techniques can be found in [44].

Insufficient research work, thus far, has been done on build orientation optimization for additive manufacturing of FGM objects. Majority of the research in build orientation optimization has focused on optimizing build time, build cost, and geometric features (such as surface quality, support volume, contact area of support, and number of layers) of single (homogeneous) material parts. Frank and Fadel [10] proposed an expert system that considered surface finish, build time, and support generation. Cheng et al. [8] presented a multi-objective approach with part accuracy as the primary objective and build time as the secondary objective. The algorithm seeks to maximize the primary objective (part accuracy) and uses the secondary objective (build time) when several orientations are within a certain range of the maximum accuracy. Hur and Lee [18] used stair-case error as their primary parameter and build time and volume of support as secondary parameters. Allen and Dutta [3] used support structure and contact area for support structure to determine the optimal orientation. Alexander et al. [2] developed an

accuracy and cost calculation model. Pandey et al. [33] proposed a multi-objective genetic algorithm to search for the Pareto solutions. A multi-step optimization framework was proposed by Verma and Rai [40] wherein they sought to minimize energy consumption, material wastage, and geometric errors. Armillotta et al. [5] proposed a two-step selection method in which near-optimal orientations are generated by former multi-objective optimization methods and the final optimal orientation is selected by a visual evaluation that is based on the criterion of the integrity of fine form details and local defects. Verma and Rai [41] developed a computational geometric approach to make critical manufacturing planning decisions in AM that involves identifying optimal build orientation based on material wastage and surface roughness.

Numerous optimization-based frameworks have been developed for build orientation selection of single material 3D printed parts. However, none of the existing frameworks consider material composition error during the printing process. The material composition error is an important criterion for additive manufacturing of FGM objects. Shin and Dutta [36] addressed this issue partially in the process planning for additive manufacturing of FGM objects. They discretized material composition in a layer into homogeneous lumps and sought to minimize the number of material change, assuming that it will reduce material composition error and improve surface finish. However, minimizing the number of material changes inherently increases the size of homogeneous lumps and hence results in a higher difference in desired and attained material distribution. Therefore, in this paper, a novel approach to compute material composition error has been proposed. The material composition error was used in conjunction with stair-case geometric error to solve the build orientation optimization problem.

The build orientation cost function evaluation involves several expensive computations. Due to a computationally expensive cost function evaluations required in the overall proposed formulation, very few methods are left at our disposal to solve the formulated optimization problem. *Surrogate model* (also known as *response surface model* or *meta models*)-based optimization is one such method, where the objective function is approximated by a surrogate model, that can be used to efficiently solve such problems. The application areas for surrogate model-based optimization vary immensely, and hence various types of surrogate models have been proposed in literature. Surrogate models are typically divided into two broad categories: interpolating models such as kriging [22, 31] and radial basis functions [17, 34], and non-interpolating models such as polynomial regression and multivariate adaptive regression splines [12]. In our study, we have utilized MATLAB Surrogate Model Toolbox (MATSuMoTo) developed by Mueller [32] to enable surrogate model-based optimization. MATSuMoTo was designed to solve computationally expensive black-box global optimization problems. *Black-box optimization problems* are a class of optimization problems where an explicit mathematical and functional description of the problem is not available.

3 Overview

Figure 1 shows an overview of the overall build orientation optimization process. The absence of a standardized FGM model representation scheme mandated selection and development of an efficient and robust representation scheme. A distance function-based material representation scheme inspired by fixed reference feature-based representation [43] and distance field-based representation [7] is used for FGM model representation (Fig. 1b). This scheme allows for representing complex material distribution over any geometric shape. It also enables easy and efficient processing to formulate and solve the build orientation optimization problem.

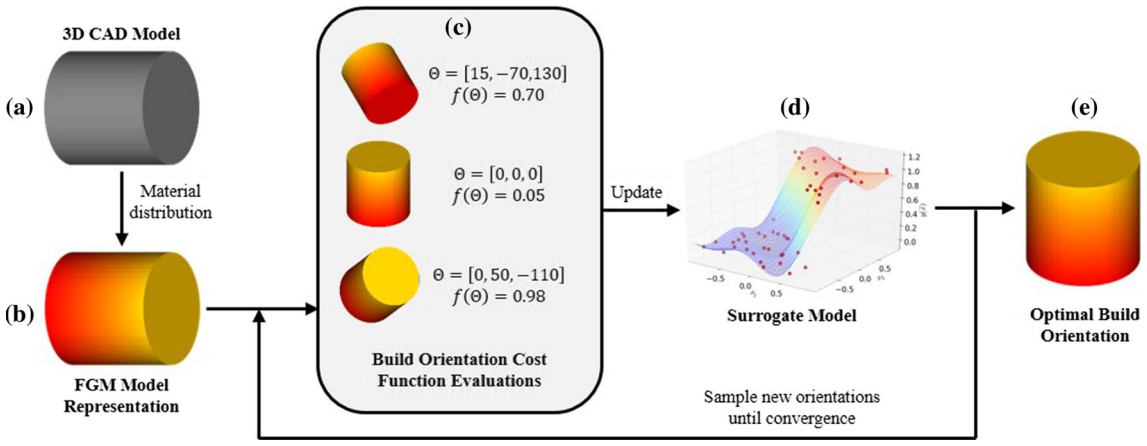

Fig. 1 An overview of the FGM object build orientation optimization process

Due to discretization and limitations of the additive processes, it is usually not possible to achieve the desired shape, surface finish, and material distribution in the printed part without errors and defects. Although there are a variety of sources of error, in this paper, we focus on staircase error and material distribution error. This paper introduces a novel multi-scale random error computation for quantifying material distribution error. To this end, we define attainable material composition that portrays an estimate of material distribution achievable in printed part. It is different from the desired material composition and is defined based on the discretization due to slice height, toolpath, and printer resolution. Since the error computation over the whole volume of the model would involve computationally expensive integration, a multi-scale random error computation approach is used to compute the material distribution error.

The build orientation optimization cost function is formulated as a weighted sum of geometric and material error. The angles representing the build orientation are regarded as design variables. The large number of computationally expensive geometric computations involved in the cost function evaluation renders the conventional gradient/Hessian-based optimization methods incapable of solving the build orientation optimization problem. Hence, a surrogate model-based optimization method [32] has been used. In this method, a minimal initial design point set representing multiple build orientations is created and evaluated to arrive at cost function values (Fig. 1c). A surrogate model is then fitted onto the dataset to generate an approximation of the cost function. New data points, based on a specified search criteria, are sampled and evaluated to progressively improve the surrogate model (Fig. 1d). The process is repeated until the stopping criteria is satisfied and an optimal build orientation is identified (Fig. 1e). Next, we outline the details pertaining to all the main components of the overview.

4 FGM: modeling and representation

Representation of an FGM model in the form of computer readable data structure is key to perform computations related to build orientation optimization. An effective data structure allows for efficient creation, modification, retrieval, and processing of the contained information. There are numerous techniques proposed for representing and modeling FGM objects [44]. For the purposes of the presented work, a distance function-based FGM representation scheme has been used. In this scheme, the object geometry is represented by a triangulated surface mesh and material composition at any point inside the object is defined as a non-negative function of distance from one or more user-defined reference geometries. The user is provided with the flexibility to define any number of references and distance functions to realize highly complex material distribution inside the object. It is important to note that the presented build orientation optimization approach is independent of the FGM representation scheme, and it could be used in conjunction with any valid representation scheme.

4.1 Data structure

A schema of the data structure used to represent FGM objects is shown in Fig. 2. The data structure includes information regarding the geometry and material of the FGM object. It could also contain optional manufacturing process specific information, such as slice height and nozzle diameter. The triangulated surface mesh geometry is stored as a half-edge data structure [23] with few additional information such as face normals for efficient retrieval and processing. To represent the material distribution of the FGM object, the information about the constituent raw materials, the reference geometries, and the non-negative distance functions are included. The desired materials composition at any point can be easily computed using such a representation as described in Section 4.2. The process specific information helps in estimating the attainable material composition at a given point.

4.2 Material composition definition

Material composition at a point $\mathbf{x}$ is defined by a vector $M_{\mathbf{x}}$ of volume fractions of constituent raw materials. The

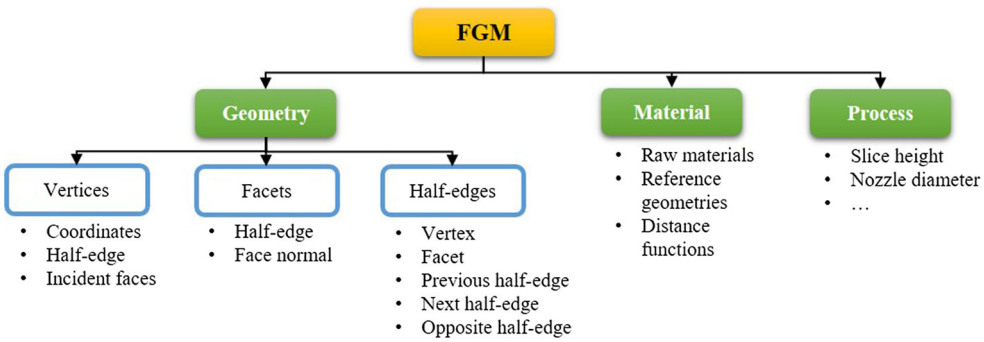

Fig. 2 A layout of the data structure of FGM model

length of the vector is same as the number of constituents. A valid material composition vector has an L_1-norm of 1, i.e., $\sum_i M_{\mathbf{x},i} = 1$ and each element of the vector is non-negative. Each point $\mathbf{x}$ has two material composition definitions – a desired composition $M^d_{\mathbf{x}}$ and an attainable composition $M^a_{\mathbf{x}}$. The desired composition is the material composition defined using the reference geometries and the distance functions. The attainable composition is the estimated material composition achievable at the corresponding point after the model has been additively fabricated (Section 5.2.1). The desired and the attainable compositions are usually different from each other due to unavoidable manufacturing errors and limitations of the AM process.

To specify the desired material distribution in the FGM object, one or more reference geometries could be defined. A reference geometry could be a point, a line, a plane, or a surface. The material composition can be defined as a vector-valued function of Euclidean distances from these references. For instance, consider a two-dimensional example shown in Fig. 3 with two reference geometries – β_1: line $x = 1$ and β_2: point $(x = 0, y = 1.5)$. Let the shortest Euclidean distances of a point $\mathbf{x}$ from these references are given by $s_{\mathbf{x},1}$ and $s_{\mathbf{x},2}$, respectively. One could define a material distribution, consisting of two materials P and Q, as polynomial functions of $s_{\mathbf{x},1}$ and $s_{\mathbf{x},2}$:

$$M^d_{\mathbf{x}} = \frac{1}{Z}[5s_{\mathbf{x},1} + s_{\mathbf{x},2}, s^2_{\mathbf{x},2}] \tag{1}$$

where $Z = 5s_{\mathbf{x},1} + s_{\mathbf{x},2} + s^2_{\mathbf{x},2}$ is the normalizing factor. The first and second coordinates of $M^d_{\mathbf{x}}$ represent the volume fraction of the constituent materials P and Q, respectively. The generated material distribution in a 2D plane is shown as a color plot in Fig. 3. In a similar fashion, material distribution can be generated in 3D inside the FGM object. A simple example of 3D cylinder with a linear gradient of materials across its axis is shown in Fig. 4. In this case, the reference geometry is the bottom planar surface of the cylinder or $z = 0$, and the material composition function is linear with respect to the Euclidean distance from the surface.

4.3 Slicing and toolpath generation

The optimal orientation (minimum error) for manufacturing of the FGM object is highly dependent on the slicing and toolpath. Here, a brief description of the approach used for slicing and toolpath generation is provided. The global positive z-axis was considered to be the build direction. The slices were created by intersecting the triangulated surface mesh geometry of the FGM model with planes perpendicular to the build direction at specific heights. For a layer thickness of h, the slicing started with the plane at height $h/2$ above the minimum z-coordinate of the surface mesh. At steps of h, new slices were created until the maximum z-coordinate was reached. The intersection between a plane and surface mesh was performed using axis-aligned bounding box (AABB) tree implemented in CGAL C++ library [4, 38]. The intersection results in a list of boundary line segments for the slice, which are then used for further processing.

A simple toolpath generation approach was followed. In this approach, a zig-zag toolpath aligned along y-axis was created for each slice. Parallel line segments with a finite width were generated to fill the 2D region enclosed within the slice. The ends were connected alternately to

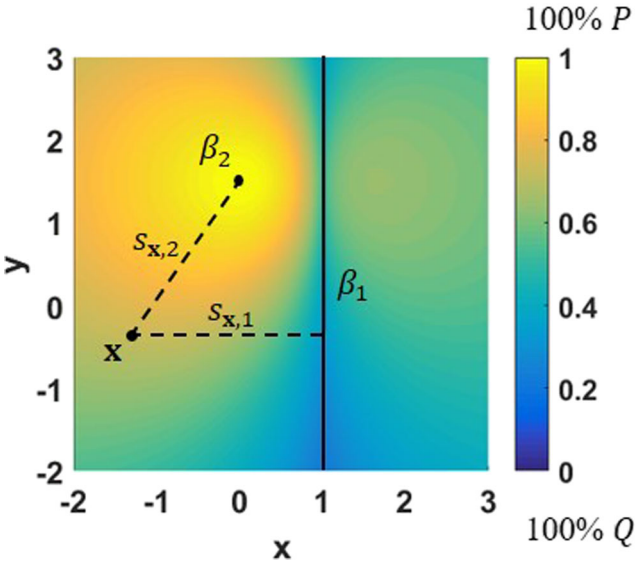

Fig. 3 An example of desired material distribution in 2D created using two reference geometries β_1 and β_2

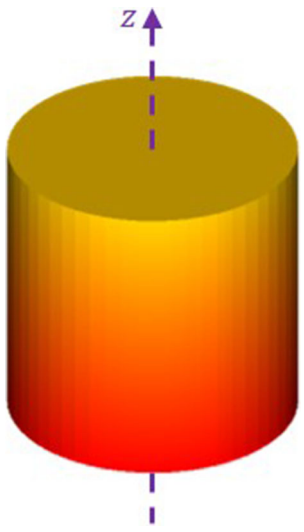

Fig. 4 A simple example of FGM object: cylinder with material gradient along z-axis

create a zig-zag pattern. Since the toolpath was used only to define attainable material compositions (Section 5.2.1), the non-printing segments of the toolpath were ignored, and only the printing segments were stored. The optimization techniques described in this paper is independent of the toolpath generation scheme used, and any other scheme could also be used.

5 Build orientation optimization

Build orientation is one of the key factors that influence the printed part quality, build time, support structure, and cost. As discussed in Section 2, the majority of the research for build orientation optimization focuses on homogeneous material objects. In the case of FGM object, the build orientation also directly affects the material composition quality and discretization. Hence, it is crucial to study the effects of build orientation on material distribution in FGM objects and account of material composition error in the overall build orientation optimization.

In addition to the material composition error, geometric error in additive manufacturing of the FGM objects is also considered. In this paper, equal priority is assigned to both geometric and material accuracy. Hence, the build cost function is defined as the mean of normalized geometric error and normalized material composition error with equal weights. However, the relative weights can be adjusted to reflect the importance of one over the other based on the application and the process used. In addition, other key attributes, such as support structure and print time, can also be augmented into the build cost function.

5.1 Geometric error

Geometric error is a well-studied subject in additive manufacturing with many methodologies developed that focus on various sources contributing to the overall error. Following two errors are the most studied sources of geometric errors in research literature:

1. Staircase effect: The layer-wise manufacture of the object in 3D printing causes staircase effect due to finite layer thickness. It is the most studied and critical source of geometric error that appears along the inclined or curved surfaces. Often, the printed object requires post-processing, such as polishing, to remove the unevenness caused by staircase effect. The layer thickness and the local inclination of the surface directly affect the staircase error. Since the layer thickness cannot be lowered beyond the limits of the machine, the goal of the build orientation optimization is usually to adjust the inclination of the surface relative to the build direction in a global sense.
2. Support contact area: In many additive manufacturing processes like SLA and FDM, a support structure is necessary to provide support to the overhanging regions of the design. Support structures influence the surface roughness of the manufactured object. After printing, time-consuming and uneconomical post-processing is required to remove the support structure and finish the surface. Hence, minimizing support contact area is another vital factor in reducing geometric error.

There are few other sources of geometric error, such as tessellation, distortion, shrinkage, and the trapped volumes due to surface tension. However, in this study, we will mainly focus on the staircase effect. The staircase error was computed as the volume of unwanted under-deposition and over-deposition of material (see Fig. 5). The erroneous volume can be estimated by accumulating volumes of under- and over-depositions caused by each triangular facet on the surface of the model. The erroneous volume ν^k for k^{th} triangular facet is calculated as follows:

$$\nu^k = \begin{cases} \lambda \delta^k A^k, & \text{if } |\hat{\eta}_z^k| = 1 \\ \frac{1}{2}\lambda \hat{\eta}_z^k A^k, & \text{otherwise} \end{cases} \tag{2}$$

where,

$$\delta^k = |\lfloor r^k + 0.5 \rfloor - r^k|, \tag{3}$$

$$r^k = \frac{z^k - z_{\min}}{\lambda}, \tag{4}$$

z^k is the z-coordinate of k^{th} triangle with face normal along z-axis, $z_{\min}$ is the bounding box minima in z-direction, λ is the slice thickness (constant for all slices), A^k is the area of k^{th} triangular facet, and $\hat{\eta}_z^k$ is the z-component of its unit face normal. The accumulation of erroneous volumes over all facets gives the total geometric error $\epsilon_G = \sum_k \nu^k$.

5.2 Material composition error

In addition to geometric accuracy, material composition accuracy is another critical factor in additively fabricated FGM object. Conventional process planning steps, such as

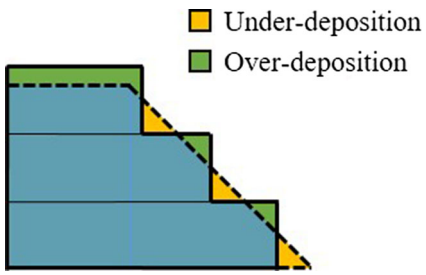

Fig. 5 Staircase error in additive manufacturing

orientation optimization, support generation, slicing, and toolpath generation, are mainly based on geometry and do not consider their effects on the material distribution in the object. In this paper, a novel methodology is proposed to quantify the material composition error in additive manufacturing of the FGM objects. The manufacturing process parameters are used to discretize the material composition to simulate the as-printed part. Material composition error is then computed by evaluating the difference of the desired material composition and the attainable material composition after discretization. The material composition error is used in conjunction with the geometric error to identify an optimal build orientation for FGM objects.

5.2.1 Material composition discretization

As shown in Fig. 6, it was assumed that the additive manufacturing equipment deposits material as a circular sweep on continuous portions of the toolpath and could achieve arbitrary grading of material composition along the length of the toolpath. The assumption is reasonable for the recent state-of-the-art multi-material 3D printers and processes. In these processes, the material is deposited as a continuous flow of molten ingredients, which forms a circular sweep shape. A remarkable characteristic of these processes is that they can continuously change the material composition ejected from the nozzle while printing. However, at a given instant of time, the bulk of the ejected material has a uniform composition. Hence, the material distribution across the cross-section of the toolpath was considered to be uniform and same as the desired material composition at the center of the circular cross-section. This discretization of material was used as the primary source of material composition error, since the desired material composition often varies across the cross-section. Material discretization depends on slicing and toolpath, which are both affected by build orientation. Therefore, by optimizing the build orientation, it is possible to minimize the material composition error between the desired material distribution and the actual material printed.

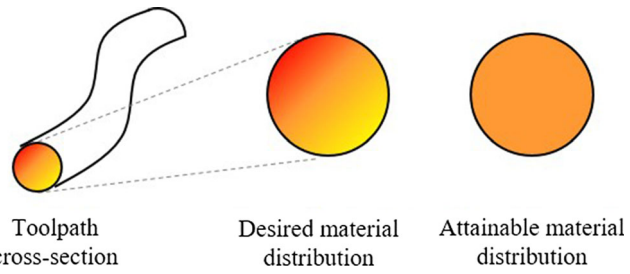

Fig. 6 Material composition discretization across the toolpath cross-section

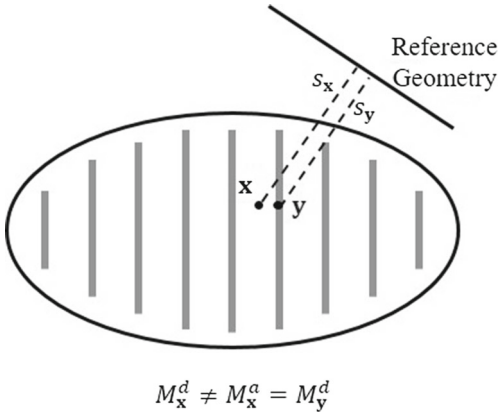

Fig. 7 The attainable material composition at a point **x** is same as the desired material composition at the closest point **y** on the toolpath

5.2.2 Multi-scale random error computation

The material composition error at a point **x** is given by ℓ^2-norm of the difference between desired material composition ($M_{\mathbf{x}}^d$) and attainable material composition ($M_{\mathbf{x}}^a$). The desired material composition was computed based on the reference geometries and distance functions as described in Section 4.2. The attainable material composition was estimated using the material discretization assumption. It was assumed that the actual material deposited at **x** would have the composition same as of the nearest point on a toolpath segment. Hence, the attainable material composition was calculated by first finding the point **y** on the toolpath that is nearest to **x** and then computing the desired material composition at **y** (see Fig. 7). Therefore, $M_{\mathbf{x}}^a = M_{\mathbf{y}}^d$.

Computing the aggregate material composition error of the whole FGM model requires a computationally expensive and prohibitive integration over the 3D domain. In order to balance an effective estimate of the material composition error and the computational cost, a multi-scale random error approach is proposed. In this approach, random points

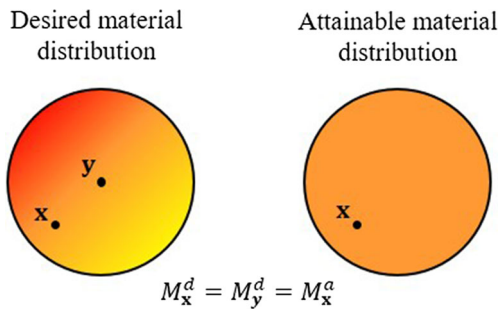

Fig. 8 A single point is often incapable of capturing material composition error in its local neighborhood. In this example, the material composition error at **x** would be zero, although the attainable material composition in its neighborhood is not error-free

were sampled in the 3D space, and the material error was computed at those points. However, often a point might not be an effective representative of the local material error in its neighborhood as shown in Fig. 8. Therefore, the error was computed at four different scales. For defining the scales, we assume a uniform axis-aligned voxelization of the FGM model. In our study, the edge length of the voxels was chosen to be $1/8^{th}$ of the layer thickness λ. The material composition error in a voxel was defined to be the material composition error at its centroid. To capture the local characteristics of the error, the four different scales (Fig. 9) were chosen as follows:

1. Single voxel: This is the smallest scale, where the material composition error is simply computed at the centroid of the selected voxels.
2. 6-connected voxels: At this scale, all the face neighbors (voxels sharing a face) of the selected voxels are considered in the material error computation as well.
3. 18-connected voxels: Face neighbors and edge neighbors are both included in the error computation at this scale.
4. 26-connected voxels: At this scale, all the neighbors of the voxels, including face, edge, and corner neighbors, are considered in the error computation.

A unique set of voxels was randomly selected for each scale. For each scale (except the first one), in addition to computing the material composition error at the centroid of the selected voxels, the error was also computed at the centroid of their neighbors. The error from all the voxels at all scales was then accumulated as a sum and divided by the total number of voxels for obtaining a mean multi-scale material composition error ϵ_M.

$$\epsilon_M = \frac{1}{N}\sum_{i=1}^{N} \|M_i^d - M_i^a\| \tag{5}$$

where $\|\cdot\|$ is ℓ^2-norm, N is the total number of voxels (including neighbors), and M_i^d and M_i^a are desired and attainable material composition at the i^{th} voxel centroid, respectively. Note that, in our study, we varied the number of randomly selected voxels for error computation based on the number of layers (q) in a particular orientation of the FGM model. The number of voxels for each scale was selected such that the total number of voxels N was around $\sim 150q$.

5.3 Optimization problem formulation

An orientation of the FGM model is described by a vector of three angles $\Theta = [\theta_x, \theta_y, \theta_z]$ corresponding to rotations about the three coordinate axes. The default orientation was assumed to be a zero-valued vector $\Theta_0 = [0, 0, 0]$. For any orientation, the rotations are performed on the whole FGM model, including its vertices, face normals, and reference geometries. Due to the non-commutative nature of the rotations, it must be carried out in a specified order – rotation about z-axis, followed by y-axis, and finally x-axis. The homogeneous affine rotation matrices about each of the axes are given as follows:

$$R_x(\theta_x) = \begin{bmatrix} 1 & 0 & 0 & 0 \\ 0 & \cos(\theta_x) & -\sin(\theta_x) & 0 \\ 0 & \sin(\theta_x) & \cos(\theta_x) & 0 \\ 0 & 0 & 0 & 1 \end{bmatrix} \tag{6}$$

$$R_y(\theta_y) = \begin{bmatrix} \cos(\theta_y) & 0 & \sin(\theta_y) & 0 \\ 0 & 1 & 0 & 0 \\ -\sin(\theta_y) & 0 & \cos(\theta_y) & 0 \\ 0 & 0 & 0 & 1 \end{bmatrix} \tag{7}$$

$$R_z(\theta_z) = \begin{bmatrix} \cos(\theta_z) & -\sin(\theta_z) & 0 & 0 \\ \sin(\theta_z) & \cos(\theta_z) & 0 & 0 \\ 0 & 0 & 1 & 0 \\ 0 & 0 & 0 & 1 \end{bmatrix} \tag{8}$$

The objective of the build orientation optimization is to identify an optimal orientation that minimizes the error in manufacturing of FGM object. The design variables

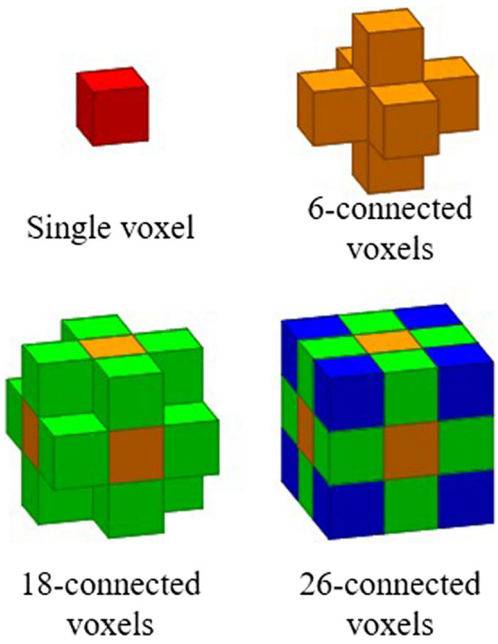

Fig. 9 The four scales chosen for multi-scale random error computations

of the optimization problem are $\Theta = [\theta_x, \theta_y, \theta_z]$. The optimization problem can be stated as follows:

$$\begin{aligned} \underset{\Theta}{\text{minimize}} \quad & f(\Theta) = w\hat{\epsilon}_G + (1-w)\hat{\epsilon}_M \\ \text{subject to} \quad & -\frac{\pi}{2} \leq \theta_x \leq \frac{\pi}{2} \\ & -\frac{\pi}{2} \leq \theta_y \leq \frac{\pi}{2} \\ & -\pi \leq \theta_z \leq \pi \end{aligned}$$

where $f(\Theta)$ is the optimization cost function given by the weighted sum of normalized geometric and material composition errors. In our study, the weight w was set to 0.5 to reflect equal importance to both geometric and material composition error. $\hat{\epsilon}_G$ and $\hat{\epsilon}_M$ are normalized form of geometric (ϵ_G) and material composition (ϵ_M) errors, respectively. Normalization was performed using initial design space described in the following section.

6 Surrogate model-based global optimization scheme

The optimization cost function computation, which involves calculation of geometric and material error, is highly computationally expensive due to a large number of 3D geometric computations involved. Some of the complex geometric tasks in cost function evaluation include slicing, toolpath generation, geometric error computation, voxelization, and numerous distance computations for desired and attainable material composition definitions. Moreover, the computational complexity escalates with lower layer thickness, intricate geometries, and complex material distributions. Therefore, we adopted a surrogate model-based optimization approach, wherein the cost function is considered as a black box problem characterized by only its input and output. How surrogate model-based optimization works is illustrated in Fig. 10. Here, the x-axis represents the design variable and the cost function is plotted on the y-axis.

In our study, we used MATLAB's surrogate modeling toolbox (MATSuMoTo) [32]. MATSuMoTo provides flexibility to choose from various types of surrogate models, initial design space generation methods, and new sample points generation methods. The basic outline of MATSuMoTo optimization process is described below.

Initial design space The algorithm starts by creating an initial design space, which in our case is an initial set of orientations, using the chosen design of experiment (DOE) scheme. Although the user has the flexibility to adjust the size of the design space, the minimum size depends on the desired surrogate model. MATSuMoTo toolbox provides three DOE strategies, namely Latin hypercube design, symmetric Latin hypercube design, and corner points design. In this paper, Latin hypercube design strategy was used to evenly distribute the initial design space over the entire domain of design variables. Once the design space of orientations is generated, geometric error and material composition error was evaluated for these orientations. The geometric error and the material composition error were normalized independently between 0 and 1. The normalization parameters were stored for further computations. The weighted average (equal weights in our study) of the normalized errors yield the cost function value.

Surrogate model Next, a surrogate model was mapped on the initial design space data to create an analytical function mapping the design variables to the cost function values. The choice of the surrogate model is application specific and is based on methods such as radial basis functions (RBF) models, Kriging models, and polynomial regression models. MATSuMoTo toolbox offers fifteen different types of surrogate models, which are designed using one or more of the above-mentioned methods. In this paper, the cubic RBF surrogate model was used. The cubic RBF model does not require shape factor tuning and hence provides fast computation. It also delivers high performance and robustness for small sample sizes [20].

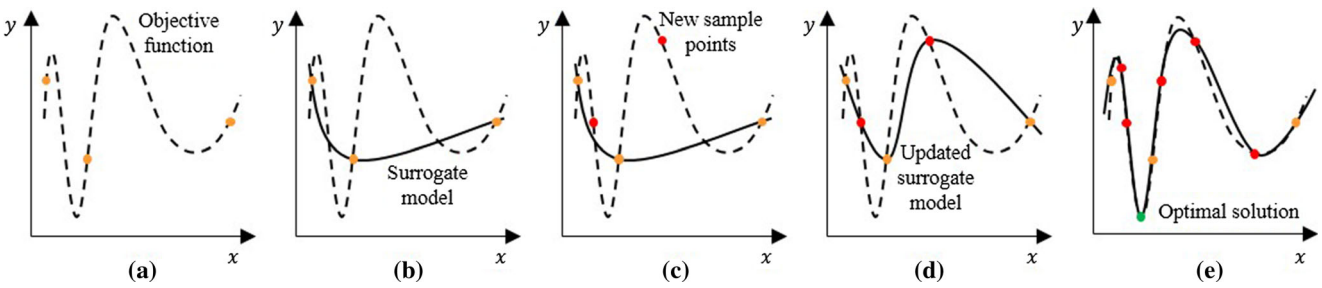

Fig. 10 One-dimensional example of surrogate-model-based optimization: **a** Objective cost function (**- - -**) and initial design space (●); **b** Surrogate model (—) mapped to initial design space; **c** New sample points (●) generated in the next iteration; **d** Surrogate model updated based on information from new sample points; and **e** After iteratively updating and achieving convergence, optimal solution (●) obtained

Selection of new samples In this step, a new set of sample orientations are generated, and the geometric and material composition errors were evaluated at the newly generated orientations. The errors were then scaled using the pre-stored normalizing parameters, and the cost function was computed. Note that the normalized errors can overshoot the [0, 1] range in this case. The surrogate model was progressively improved using the new data samples. The user can define the desired number of sample points to be selected in each iteration. MATSuMoTo toolbox provides three different approaches for new sample point generation – CANDloc, CANDglob, and Surrogate model minima. Due to the effectiveness of CANDglob method in avoiding local minima, it was used in our study to generate five new sample points at each iteration. In this method, few candidate points are generated by small perturbations of the current minima of the surrogate model and the remaining by uniformly sampling points from the whole domain.

Iterations and termination The algorithm compares the cost function values of the new sample points and asses the stopping criteria. The algorithm iterates through the process and progressively improves the surrogate model until the stopping criteria are satisfied. In this paper, two stopping criteria are used. Either one of them has to be satisfied to terminate the program. First stopping criterion is satisfied if the improvement in the optimal cost function value is less than 10^{-4} for 10 consecutive iterations ($\sim$50 function evaluations). Second is satisfied when the total number of function evaluations including the initial design space exceeds a pre-set limit T. In the test case studies presented in this paper, T was set to between 300–900. The initial design space size was chosen to be $T/6$ for all the test cases.

7 Results and discussions

Several test cases were designed with varying degree of geometric and material complexity to assess the developed methodology. Five test cases are presented here. The first two test cases have simple geometry and material distribution that allows for intuitive prediction of optimal build orientation. This enables verification and demonstration of the correctness of our system. The remaining test cases have complex geometry and material distribution establishing the effectiveness and applicability of the proposed approach. These test cases encompass FGM products for real applications in various domains, such as consumer products (mouse), healthcare (dental implant), and aerospace (propeller).

Test case 1 A cube with side-length $a = 50$ mm was created with two materials (Fig. 11a). The material composition varied linearly along the space diagonal of the cube. In the initial axis-aligned orientation, the desired material composition $M^d_{\mathbf{x}}$ at a point $\mathbf{x}$ inside the cube is given as $\frac{1}{\sqrt{3}a}[s_{\mathbf{x}}, \sqrt{3}a - s_{\mathbf{x}}]$, where $s_{\mathbf{x}}$ is the distance of point $\mathbf{x}$ from the plane passing through origin [0, 0, 0] and normal to the space diagonal direction [1, 1, 1].

The build orientation cost function is formulated with equal importance to geometric and material accuracy. Therefore, the expected optimal orientation is likely to keep the faces of the cube either parallel or perpendicular to the build direction to reduce geometric error. It is also likely to orient the cube such that the material grading direction (space diagonal) is aligned with the toolpath as much as possible to minimize material composition error due to discretization. Note that in our approach, the zig-zag toolpath pattern is generated with y-direction as the major axis. The results of the optimization process are shown in Fig. 11a. As expected, the optimal build orientation of $\Theta = [90, 38, -180]$ `degrees` ensures that all the cube faces are either parallel or perpendicular to the build direction (z-axis) and the material gradient direction in each slice is majorly aligned with y-axis. Two next best orientations are also presented, along with three least favorable orientations evaluated during surrogate model-based optimization. The convergence plot of the minimum function value with the number of function evaluations is also presented.

Test case 2 A cylinder with radius $r = 25$ mm and height $h = 50$ mm was created with linearly grading material along its central axis (Fig. 11b). The initial orientation of the cylinder has its central axis aligned with z-axis and its bottom face coplanar with xy-plane. The desired material composition $M^d_{\mathbf{x}}$ at a point $\mathbf{x} = [x, y, z]$ inside the cylinder in this orientation is given as $\frac{1}{h}[z, h - z]$. Intuitively, the optimal build orientation would be same as the initial orientation with build direction along z-axis. In this orientation, the tessellated triangular faces on the surface are either parallel or perpendicular to the build direction for minimal geometric error. Also, since the material composition is constant in any plane perpendicular to build direction, the only source of material discretization error would be the finite slice thickness.

The results of the optimization are shown in Fig. 11b. The optimal orientation is indeed found to be very close to the initial orientation. The next top two orientations are also found to be very similar to the initial orientation. The bottom three orientation samples with highest cost function values are also presented. The convergence plot of optimal cost function value is also shown.

Test case 3 A FGM mouse cover with two constituent materials was created (Fig. 11c). The desired material composition varied linearly with the distance from the

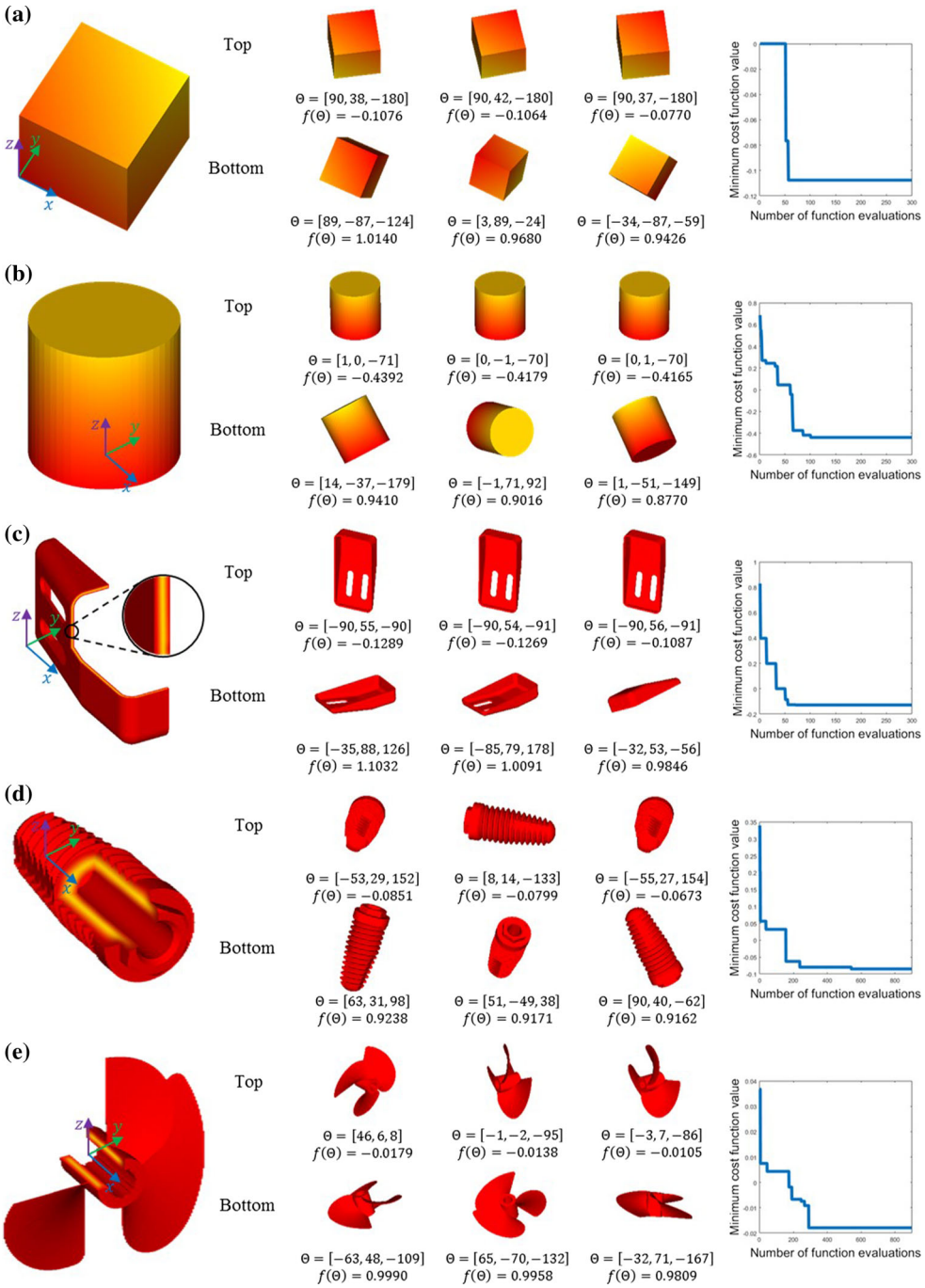

Fig. 11 Results for the five test cases (**a**–**e**) are presented. Section views of (**c**–**e**) show the material distribution inside the models. The **top** three and the **bottom** three orientations in terms of cost function values among the orientations evaluated during surrogate model-based optimization are shown. The convergence plots for the optimization are also included

boundary surface of the cover. Hence, for a point **x** inside the cover, the desired material composition is given as $M_{\mathbf{x}}^{d} = [\tau_{\mathbf{x}}, 1 - \tau_{\mathbf{x}}]$, where $\tau_{\mathbf{x}} = s_{\mathbf{x}}/s_{\text{ub}}$, $s_{\mathbf{x}}$ is the shortest distance of point **x** from the boundary, and s_{ub} is an upper bound of $s_{\mathbf{x}}$ used as normalizing factor. One-half of the smallest edge-length of the axis-aligned bounding box (AABB) is used as s_{ub} in our study. Figure 11c shows the results of the optimization process with top three and bottom three build orientations based on the cost function evaluations during the optimization process. The convergence plot is also presented in the figure. The optimal cost function value obtained was −0.1289.

Test case 4 A FGM model of dental implant was created (Fig. 11d). The desired material composition was a function of the distance from the boundary surface of the implant. It is given as $M_{\mathbf{x}}^{d} = [\tau_{\mathbf{x}}^{1.5}, 1 - \tau_{\mathbf{x}}^{1.5}]$, where $\tau_{\mathbf{x}} = s_{\mathbf{x}}/s_{\text{ub}}$, $s_{\mathbf{x}}$ is the shortest distance of a point **x** inside the dental implant from its boundary, and s_{ub} is one-half of the smallest edge-length of AABB of the implant model. The top three

and bottom three orientations that were evaluated during the optimization process are shown in Fig. 11d with optimal cost function value of -0.0851.

Test case 5 A FGM propeller model was used as one of the test cases for our experiments (Fig. 11e). The desired material composition inside the propeller was a function of the distance from the its boundary, given as $M^d_{\mathbf{x}} = [\tau^{2.5}_{\mathbf{x}}, 1-\tau^{2.5}_{\mathbf{x}}]$, where $\tau_{\mathbf{x}} = s_{\mathbf{x}}/s_{\text{ub}}$, $s_{\mathbf{x}}$ is the shortest distance of a point $\mathbf{x}$ inside the propeller from its boundary, and s_{ub} is an upper bound of $s_{\mathbf{x}}$ defined as one-half of the smallest edge-length of AABB. The results of the optimization are shown in Fig. 11e. The optimal build orientation achieves the cost function value of -0.0179. The figure also shows the next top two orientations and bottom three orientations based on cost function values among all the samples evaluated during surrogate model-based optimization.

The test cases demonstrate the applicability and effectiveness of our approach in identifying the optimal build orientation for FGM models. The convergence plots show that the surrogate model-based optimization method can converge to the minima of the cost function with a small number of function evaluations. This allows for efficient estimation of optimal build orientation although the cost function evaluations are computationally expensive.

8 Conclusions and future research

The quality of the printed part in additive manufacturing is profoundly impacted by the build orientation used for fabricating the part. The severity of this influence increases for functionally graded material fabrication since the build orientation not only affects the geometric accuracy of the part but also affects the material distribution within the part. In this paper, a novel optimization approach was developed to identify an optimal build orientation that minimizes both geometric and material composition error. A distance-based FGM modeling scheme was implemented to represent and encode the desired material distribution within the part. Using this representation, the error in material composition was captured by quantifying the difference between desired and attainable material distribution. The cost function formulated for the minimization problem considered both geometric error and material composition error. The optimization problem was solved using surrogate model-based optimization method that accelerates the process by strategically choosing useful samples in the design space in each successive iterations. Using surrogate-based optimization, the optimal build orientation can be found with a small number of computationally expensive cost function evaluations.

In this work, the primary source of material error was considered to be the discretization across the cross-section of the toolpath. However, in practice, the overall material error is also dependent on the additive manufacturing equipment's ability to vary material composition along the toolpath. In this paper, it was assumed that the equipment could produce arbitrarily complex material composition variation along the toolpath. Several existing FGM printers can only mix materials in discrete fractional quantities rather than in a continuous manner. Therefore, further study is required to consider the discretization of material composition along the toolpath based on equipment specific limitations. Moreover, the developed approach only considers nozzle-extrusion-based processes such as fused deposition modeling. Studying other processes and incorporating them into our optimization framework or developing a similar framework for those processes is an exciting avenue of future work.

The computational framework developed in this paper successfully represents the functionally graded objects and optimizes the build orientation to minimize the geometric and material composition error. However, it is computationally very expensive and hence limits user's ability to evaluate a large number of different orientations in the optimization process efficiently. By incorporating parallel programming, the issue can be largely resolved. Since evaluating different orientations are not inter-dependent and the computation for individual slices can also be handled independently, therefore parallel computation could drastically reduce the required execution time and benefit the overall optimization process. Another possible direction of future work is extending the framework for process planning of additive manufacturing of functionally graded materials. An adaptive slicing and contour-based toolpath planning can also be implemented to further broaden the applicability of our work and improve the material composition error quantification scheme.

References

1. Ahn SH, Montero M, Odell D, Roundy S, Wright PK (2002) Anisotropic material properties of fused deposition modeling abs. Rapid Prototyp J 8(4):248–257
2. Alexander P, Allen S, Dutta D (1998) Part orientation and build cost determination in layered manufacturing. Comput Aided Des 30(5):343–356
3. Allen S, Dutta D (1994) On the computation of part orientation using support structures in layered manufacturing. In: Proceedings of solid freeform fabrication symposium, university of texas at austin, austin, TX, June, pp 259–269
4. Alliez P, Tayeb S, Wormser C (2017) 3D fast intersection and distance computation. In: CGAL User and Reference Manual, 4.10 edn. CGAL Editorial Board. http://doc.cgal.org/4.10/Manual/packages.html#PkgAABB_treeSummary

5. Armillotta A, Cavallaro M, Minnella S (2013) A tool for computer-aided orientation selection in additive manufacturing processes. In: Proceedings of of the 6th international conference on advanced research in virtual and rapid prototyping, pp 469–475
6. Bikas H, Stavropoulos P, Chryssolouris G (2016) Additive manufacturing methods and modelling approaches: a critical review. Int J Adv Manuf Technol 83(1–4):389–405
7. Biswas A, Shapiro V, Tsukanov I (2004) Heterogeneous material modeling with distance fields. Comput Aided Geom Des 21(3):215–242
8. Cheng W, Fuh J, Nee A, Wong Y, Loh H, Miyazawa T (1995) Multi-objective optimization of part-building orientation in stereolithography. Rapid Prototyp J 1(4):12–23
9. Dutta D (1998) An approach to modeling & representation of heterogeneous objects. Ann Arbor 6(48):109–2125
10. Frank D, Fadel G (1995) Expert system-based selection of the preferred direction of build for rapid prototyping processes. J Intell Manuf 6(5):339–345
11. Frazier WE (2014) Metal additive manufacturing: a review. J Mater Eng Perform 23(6):1917–1928
12. Friedman JH (1991) Multivariate adaptive regression splines. Ann Stat 19(1):1–67
13. Gao W, Zhang Y, Ramanujan D, Ramani K, Chen Y, Williams CB, Wang CC, Shin YC, Zhang S, Zavattieri PD (2015) The status, challenges, and future of additive manufacturing in engineering. Comput Aided Des 69:65–89
14. Gibson I, Rosen DW, Stucker B et al (2010) Additive manufacturing technologies, vol 238. Springer, Berlin
15. Guo N, Leu MC (2013) Additive manufacturing: technology, applications and research needs. Front Mech Eng 8(3):215–243
16. Gupta V, Tandon P (2015) Heterogeneous object modeling with material convolution surfaces. Comput Aided Des 62:236–247
17. Gutmann HM (2001) A radial basis function method for global optimization. J Glob Optim 19(3):201–227
18. Hur J, Lee K (1998) The development of a cad environment to determine the preferred build-up direction for layered manufacturing. Int J Adv Manuf Technol 14(4):247–254
19. Jackson T, Liu H, Patrikalakis N, Sachs E, Cima M (1999) Modeling and designing functionally graded material components for fabrication with local composition control. Mater Des 20(2):63–75
20. Jin R, Chen W, Simpson TW (2001) Comparative studies of metamodelling techniques under multiple modelling criteria. Struct Multidiscip Optim 23(1):1–13
21. Jin Y-a, He Y, Fu J-z, Gan W-f, Lin Z-w (2014) Optimization of tool-path generation for material extrusion-based additive manufacturing technology. Addit Manuf 1:32–47
22. Jones DR, Schonlau M, Welch WJ (1998) Efficient global optimization of expensive black-box functions. J Glob Optim 13(4):455–492
23. Kettner L (1998) Designing a data structure for polyhedral surfaces. In: Proceedings of the fourteenth annual symposium on computational geometry. ACM, pp 146–154
24. Kieback B, Neubrand A, Riedel H (2003) Processing techniques for functionally graded materials. Mater Sci Eng A 362(1):81–106
25. Ko H, Moon SK, Hwang J (2015) Design for additive manufacturing in customized products. Int J Precis Eng Manuf 16(11):2369–2375
26. Kou X, Tan S (2005) A hierarchical representation for heterogeneous object modeling. Comput Aided Des 37(3):307–319
27. Le Bourhis F, Kerbrat O, Hascoët JY, Mognol P (2013) Sustainable manufacturing: evaluation and modeling of environmental impacts in additive manufacturing. Int J Adv Manuf Technol 69(9-12):1927–1939
28. Liu H, Maekawa T, Patrikalakis N, Sachs E, Cho W (2004) Methods for feature-based design of heterogeneous solids. Comput Aided Des 36(12):1141–1159
29. Mahamood RM, Akinlabi ET (2017) Types of functionally graded materials and their areas of application. In: Functionally graded materials. Springer, pp 9–21
30. Mahamood RM, Akinlabi ET, Shukla M, Pityana S (2012) Functionally graded material: an overview. In: Proceedings of the world congress on engineering 2012 Vol III (WCE 2012), London, UK
31. Martin JD, Simpson TW (2005) Use of kriging models to approximate deterministic computer models. AIAA J 43(4):853–863
32. Müller J (2014) Matsumoto: the matlab surrogate model toolbox for computationally expensive black-box global optimization problems. arXiv:1404.4261
33. Pandey PM, Thrimurthulu K, Reddy NV (2004) Optimal part deposition orientation in fdm by using a multicriteria genetic algorithm. Int J Prod Res 42(19):4069–4089
34. Powell MJ (1992) The theory of radial basis function approximation. Adv Numer Anal 2:105–210
35. Reimanis IE (2004) Functionally graded materials. In: Handbook of advanced materials, p 465
36. Shin KH, Dutta D (2001) Constructive representation of heterogeneous objects. J Comput Inf Sci Eng 1(3):205–217
37. Strano G, Hao L, Everson RM, Evans KE (2013) A new approach to the design and optimisation of support structures in additive manufacturing. Int J Adv Manuf Technol 66(9):1247–1254
38. The CGAL Project (2017) CGAL user and reference manual, 4.10 edn. CGAL Editorial Board. http://doc.cgal.org/4.10/Manual/packages.html
39. Vaezi M, Seitz H, Yang S (2013) A review on 3d micro-additive manufacturing technologies. Int J Adv Manuf Technol 67(5–8):1721–1754
40. Verma A, Rai R (2013) Energy efficient modeling and optimization of additive manufacturing processes. In: Solid freeform fabrication symposium, austin, TX, pp 231–241
41. Verma A, Rai R (2014) Computational geometric solutions for efficient additive manufacturing process planning. In: ASME 2014 international design engineering technical conferences and computers and information in engineering conference, american society of mechanical engineers, pp v01AT02a043–v01AT02a043
42. Verma A, Rai R (2017) Sustainability-induced dual-level optimization of additive manufacturing process. Int J Adv Manuf Technol 88(5–8):1945–1959
43. Wu X, Liu W, Wang MY (2008) A cad modeling system for heterogeneous object. Adv Eng Softw 39(5):444–453
44. Zhang B, Jaiswal P, Rai R, Nelaturi S (2016) Additive manufacturing of functionally graded objects: a review. In: ASME 2016 international design engineering technical conferences and computers and information in engineering conference. American Society of Mechanical Engineers, pp v01AT02a045–v01AT02a045
45. Zhang Y, Bernard A, Harik R, Karunakaran K (2017) Build orientation optimization for multi-part production in additive manufacturing. J Intell Manuf 28(6):1393–1407